

# Wide Head T-Shaped Gate Process for Low-Noise AlGaN/GaN HEMTs

Hyung Sup Yoon, Byoung Gue Min, Jong Min Lee, Dong Min Kang, Ho Kyun Ahn, Hae Cheon Kim, and Jong Won Lim

IT Components & Materials Research Laboratory, Electronics and Telecommunications Research Institute,  
218 Gajeong-ro, Yuseong-gu, Daejeon 305-700, Republic of Korea  
E-mail: hsyoon@etri.re.kr, Phone: +82-42-860-5602

**Keywords:** AlGaN/GaN HEMTs, Wide Head T-shaped Gate, Minimum Noise Figure

## Abstract

Low-noise performance AlGaN/GaN HEMTs by using wide head T-shaped gate process have been fabricated on semi-insulating SiC substrate. The devices with gate-length ( $L_g$ ) of 0.18  $\mu\text{m}$  and wide gate head of 1.07  $\mu\text{m}$  exhibited a transconductance of 270 mS/mm, cutoff frequency ( $f_T$ ) of 45 GHz, and maximum oscillation frequency ( $f_{\text{max}}$ ) of 137 GHz. Minimum noise figure ( $\text{NF}_{\text{min}}$ ) of 0.81 dB and associated gain ( $G_a$ ) of 12.1 dB were achieved at 10 GHz on these devices under condition of  $V_{\text{ds}} = 5$  V and  $I_{\text{ds}} = 87$  mA/mm.

## INTRODUCTION

GaN-based high electron mobility transistors (HEMTs) have demonstrated not only high-power and -frequency, but also low-noise performances with robustness and power-handling capability [1–2], which eliminates the need for additional protection circuits in front-end receiver applications [3]. To date, most of microwave noise studies on GaN-based HEMTs [2, 3–6] have been reported for the conventional T-shape gated devices with the reduced-gate length ( $L_g$ ) and -source to drain spacing ( $L_{\text{sd}}$ ). In order to improve the microwave noise performance of these devices, it is necessary to reduce the parasitic gate resistance ( $R_g$ ) as well the  $L_g$  and  $L_{\text{sd}}$  [7].

In this work, we fabricated the 0.18  $\mu\text{m}$  gate-length AlGaN/GaN HEMTs on SiC with a wide head T-shaped gate developed by using two step electron-beam lithography. The DC, RF and microwave noise performance on these devices have been investigated. The fabricated devices exhibited the minimum noise figure of 0.81 dB and associated gain of 12.1 dB at 10 GHz.

## DEVICE STRUCTURE AND FABRICATION PROCESS

The AlGaN/GaN HEMT hetero-structure was grown on 4-inch SiC substrate using metal-organic chemical vapor deposition (MOCVD). The epitaxial layer stack consists of a nucleation layer, 2  $\mu\text{m}$  of Fe-doped GaN buffer layer and a barrier layer of 25 nm-thick  $\text{Al}_{0.25}\text{Ga}_{0.75}\text{N}$ .

A wide head T-shaped gate process and GaN HEMT device fabrication flow are shown in Fig. 1.

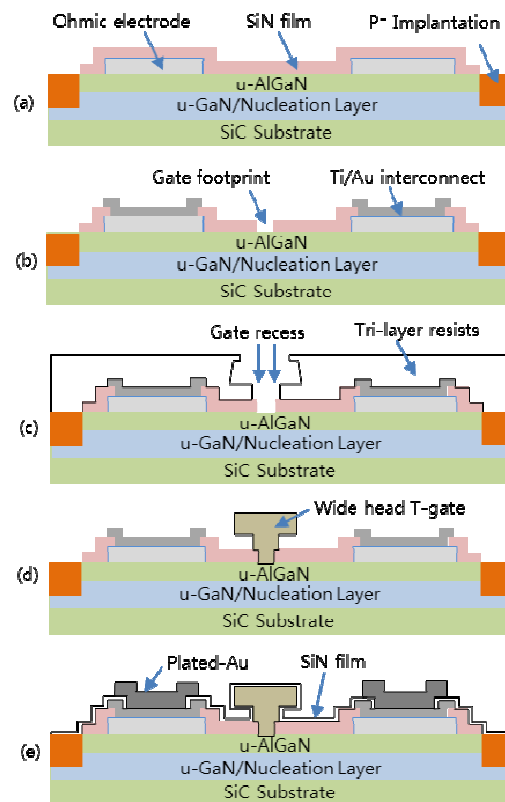


Fig. 1. Wide head T-shaped gate process and GaN HEMT device fabrication flow.

The device fabrication started with Ti/Al/Ni/Au ohmic metallization, followed by rapid thermal annealing (RTA) at 900  $^{\circ}\text{C}$  for 30 sec (Fig. 1(a)). The ohmic contact resistance of 0.35  $\Omega\cdot\text{mm}$  with channel sheet resistance of 400  $\Omega/\text{square}$  was extracted by transmission line method (TLM) measurement. Device isolation was carried out by  $\text{P}^+$  ion implantation (Fig. 1(a)). Then, 50 nm-thick SiN layer was deposited using plasma-enhanced chemical vapor deposition (PECVD). The first metal-interconnections with ohmic contacts were formed by evaporation of Ti and Au metal

after etching SiN layer (Fig. 1(b)). The wide head T-shaped gate process was performed by using two-step electron-beam lithography. A gate footprint of  $0.18 \mu\text{m}$  was first formed by e-beam exposure in PMMA resist and the SiN layer underneath the gate pattern was etched by reactive ion etching (RIE) (Fig. 1(b)). Then, a wide head T-shaped gate pattern of  $0.35 \mu\text{m}$  was directly written by another electron-beam exposure after coating PMMA/Co-polymer/PMMA triple layers and the gate recess was performed using inductively coupled plasma (ICP) etching with  $\text{BCl}_3/\text{Cl}_2$  gas (Fig. 1(c)). For gate metallization, Au/Ni metal stack with respective thickness of  $500/30 \text{ nm}$  was deposited by electron-beam evaporation and lifted off (Fig. 1(d)). A SiN PECVD film was deposited for device passivation and etched using RIE for pad contacts. Finally, air-bridged interconnections were formed with Au-plating process (Fig. 1(e)). Fig. 2 shows the inline-SEM image of the wide head T-shaped gate resist pattern after electron-beam exposure and development (Fig. 2(a)) and the cross-sectional transmission electron microscope (TEM) image of the wide head T-shaped gate electrode (Fig. 2(b)). As shown in Fig. 2(b), the wide head T-shaped gate was clearly formed by combining a narrow first gate footprint ( $L_g$ ) of  $0.18 \mu\text{m}$ , a second gate footprint of  $0.35 \mu\text{m}$ , and a wide head of  $1.07 \mu\text{m}$ . It is noticed that the overlapped area between the second footprint and the dielectric layer in this gate structure is small even with large cross-sectional gate area, which ensures lower parasitic gate resistance and capacitance.

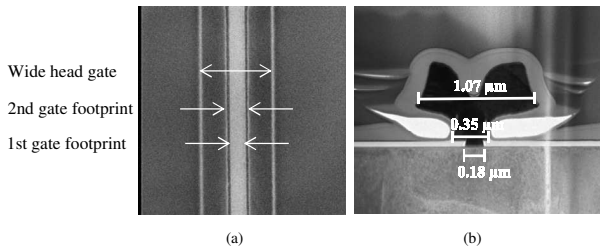


Fig. 2. Inline-SEM image of the wide head T-gate resist pattern after electron-beam exposure and development (Fig. 2(a)) and cross-sectional TEM image of the wide head T-shaped gate electrode (Fig. 2(b)).

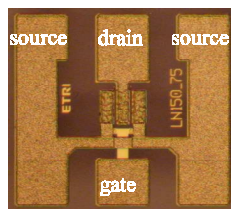


Fig. 3. Photograph of the fabricated AlGaIn/GaN HEMT devices on SiC with the wide head T-shaped gate.

Fig. 3 shows the photograph of the fabricated GaN HEMT device with the wide head T-shaped gate. The devices have the source-to-drain distance ( $L_{sd}$ ) of  $3.5 \mu\text{m}$  and the gate width of  $150 \mu\text{m}$  ( $2 \times 75 \mu\text{m}$ ).

#### RESULTS AND DISCUSSION

On-wafer DC and RF measurements were carried out using an Agilent 4155B parameter analyzer, 8510C network analyzer, and Cascade Microtech probe station. Fig. 4 shows the current-voltage (I-V) characteristics of AlGaIn/GaN HEMT devices on SiC with  $L_g$  of  $0.18 \mu\text{m}$  and  $L_{sd}$  of  $3.5 \mu\text{m}$ , where the gate-source voltage ( $V_{gs}$ ) was biased from 0 to  $-5 \text{ V}$  in steps of  $0.5 \text{ V}$ .

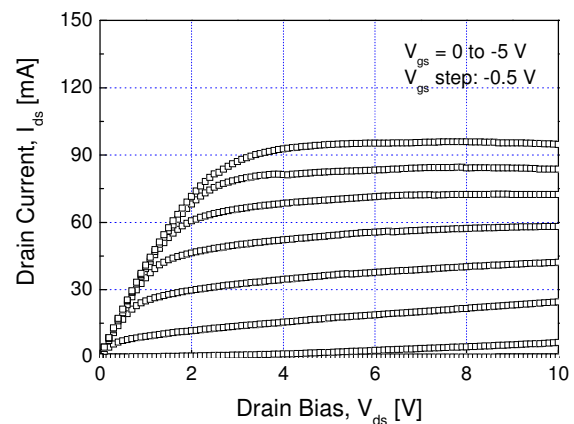


Fig. 4. Current-voltage (I-V) characteristics of the AlGaIn/GaN HEMTs with  $L_{sd}$  of  $3.5 \mu\text{m}$ ,  $L_g$  of  $0.18 \mu\text{m}$ , and gate width of  $150 \mu\text{m}$  ( $2 \times 75 \mu\text{m}$ ).

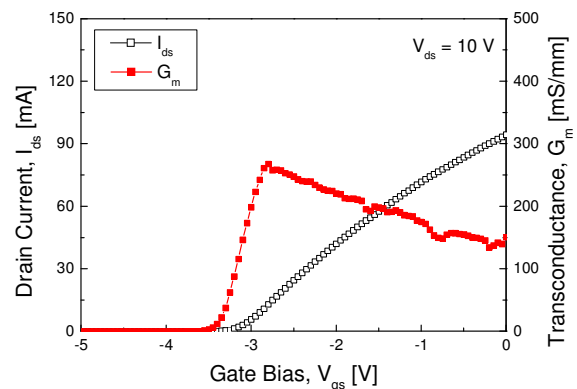


Fig. 5. Transfer characteristics of the AlGaIn/GaN HEMTs with  $L_{sd}$  of  $3.5 \mu\text{m}$ ,  $L_g$  of  $0.18 \mu\text{m}$ , and gate width of  $150 \mu\text{m}$  ( $2 \times 75 \mu\text{m}$ ). Device biased at  $V_{ds} = 10 \text{ V}$  and  $V_{gs} = -5 \sim 0 \text{ V}$ .

The devices exhibited good pinch-off characteristics. Drain saturation current density ( $I_{dss}$ ) was 626 mA/mm at  $V_{gs}$  of 0 V and  $V_{ds}$  of 10 V. The gate leakage current was as small as 0.5  $\mu$ A at  $V_{gs}$  of - 5 V and  $V_{ds}$  of 10 V. Fig. 5 shows the transfer characteristics of the device. The maximum transconductance ( $g_{max}$ ) of 270 mS/mm was measured at  $V_{gs}$  of - 2.8 V and  $V_{ds}$  of 10 V.

Fig. 6 shows the RF characteristics of the device biased at  $V_{gs}$  of - 2.65 V and  $V_{ds}$  of 10 V. As shown in Fig. 6, the cutoff frequency ( $f_T$ ) was obtained from the extrapolation of current gain ( $h_{21}$ ) to unity using - 20 dB/decade slope, and maximum oscillation frequency ( $f_{max}$ ) was extracted from the measured maximum stable/available gain (MSG/MAG) of the devices. The  $f_T$  and  $f_{max}$  for the devices are 45 and 137 GHz, respectively.

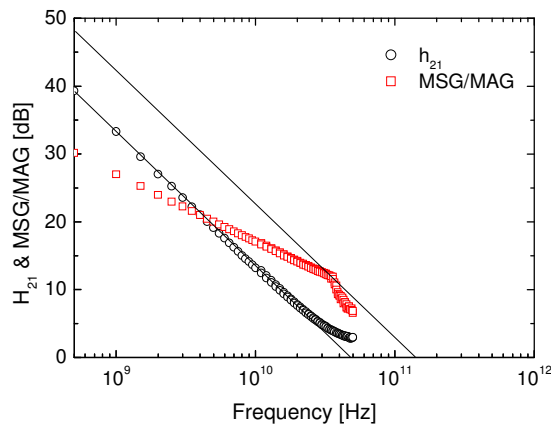


Fig. 6. RF performance of the AlGaIn/GaN HEMTs with  $L_{sd}$  of 3.5  $\mu$ m,  $L_g$  of 0.18  $\mu$ m, and gate width of 150  $\mu$ m ( $2 \times 75 \mu$ m). Device biased at  $V_{ds}$ = 10 V and  $V_{gs}$ = - 2.65 V.

Microwave noise performance of the devices with wide head T-shaped gate was measured between 4 and 18 GHz as shown in Fig. 7, using Maury noise parameter test set and Agilent 8510C network analyzer. The measurement was performed at the drain current density of 87 mA/mm under the bias conditions of  $V_{ds}$  = 5 V and  $V_{gs}$  = - 2.8 V. The devices show the minimum noise figure ( $NF_{min}$ ) of 0.81 dB and associated gain ( $G_a$ ) of 12.1 dB at 10 GHz. At 18 GHz,  $NF_{min}$  and  $G_a$  are 1.41 dB and 9.6 dB, respectively. The noise data at 10 GHz is one of the best results ever reported for the wide head T-shaped gate GaN HEMTs with similar gate length, which is attributed to the reduction of gate resistance resulting from the large cross-sectional area of the gate [7].

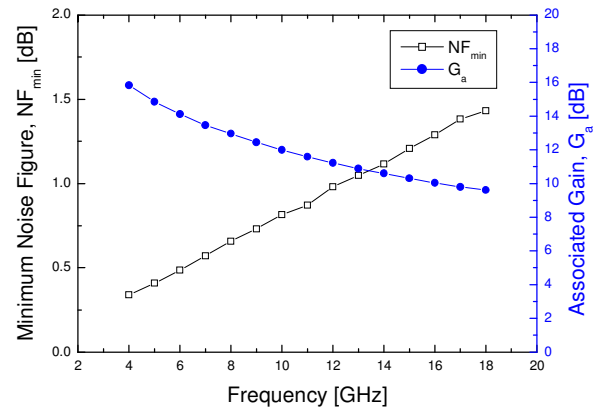


Fig. 7. Minimum noise figure ( $NF_{min}$ ) and associated gain ( $G_a$ ) as a function frequency for 0.18  $\mu$ m gate-length AlGaIn/GaN HEMTs on SiC with wide head T-shaped gate. Device biased at  $V_{ds}$ = 5 V and  $V_{gs}$ = - 2.8 V.

These results are comparable to those of  $NF_{min}$  values obtained from the conventional T-gate GaN HEMTs at 10 GHz, where the gate-length and the source-drain spacing of the devices were smaller [2, 3–6]. Therefore, the microwave noise performance for the GaN HEMT devices with wide head T-shaped gate developed in this work can be further improved with a reduction of  $L_g$  and  $L_{sd}$ .

#### CONCLUSIONS

We have fabricated the low noise 0.18  $\mu$ m gate-length AlGaIn/GaN HEMTs on SiC substrate by developing the wide head T-shaped gate process. The devices exhibited minimum noise figure of 0.81 dB at 10 GHz, which is attributed to the reduction of gate resistance due to the large cross-sectional area of the wide head T-shaped gate developed in this work. Further improvement of noise performance can be achieved by reducing  $L_g$  and the lateral scaling of GaN HEMTs with wide head T-gate.

#### ACKNOWLEDGEMENTS

This work was supported by Ministry of Trade, Industry & Energy of the Republic of Korea (Contract no. 10043806).

#### REFERENCES

- [1] T. Palacios, A. Chakraborty, S. Rajan, C. Probenz, S. Keller, S.P. DeBaars, J. Speck, and U.K. Mishra, IEEE Electron Device Lett., vol.26, no.11, pp. 781-783(2005).
- [2] N.X. Nguyen, M. Micovic, W.-S. Wong, P. Hashimoto, P. Janke, D. Harvey, and C. Nguyen, Electron Lett., vol.36, pp. 469-471(2000).
- [3] M. Rudolph, R. Behtash, K. Hirche, J. Wurfl, W. Heinrich, and G. Trankle, IEEE Trans. Microw. Theory Tech., vol.55, no.1, pp. 37-43(2007).

- [4] J.S. Moon, M. Micovic, A. Kurdoghlian, P. Kanke, P. Hasimoto, W.-S. Wong, L. McCray, and C. Nguyen, IEEE Electron Device Lett., vo.23 no.11, pp. 637-639(2002).
- [5] A. Minko, V. Hoël, S. Lepilliet, J.C. De Jaeger, Y. Cordier, F. Semond, F. Natali, and J. Massies, IEEE Electron Device Lett., vol.25, no.4, pp. 167-169(2004).
- [6] H.F. Sun, A.R. Alt, H. Benedickter, and C.R. Bolognesi, IEEE Electron Device Lett., vol.30, no.4, pp. 107-109(2009).
- [7] C.H. Oxley, Solid State Electron., vol.45, pp. 677-682(2001).

#### ACRONYMS

HEMT: High Electron Mobility Transistor  
MOCVD: Metal-Organic Chemical Vapor Deposition  
PECVD: Plasma-Enhanced Chemical Vapor Deposition  
RTA: Rapid Thermal Annealing  
ICP: Inductively Coupled Plasma  
TEM: Transmission Electron Microscope  
MSG/MAG: Maximum Stable/Available Gain